

# OBSERVATION OF LOW $x$ PHENOMENA IN HADRONIC FINAL STATES\*

GÜNTER GRINDHAMMER

Max-Planck-Institut für Physik, (Werner-Heisenberg-Institut)

80805 München, Germany

E-mail: guenterg@desy.de

(On behalf of the H1 and ZEUS collaborations)

## ABSTRACT

The expectations for and the measurements of transverse energy flows, single particle  $p_T$  spectra, and the rate of forward jets in deep inelastic  $ep$  events from the H1 and ZEUS experiments at HERA are reported and discussed. It is shown that together they offer a good chance to establish deviations from the DGLAP paradigm. At the present level of limited statistics the measurements are compatible with predictions using BFKL resummation and with the color dipole model. Models based on DGLAP evolution describe the  $p_T$  spectra and forward jets less well but are not ruled out yet.

## 1. Expectations and Observables

In deep inelastic scattering (DIS) at low  $x$  the simple picture of the quark parton model, where a virtual photon interacts with a point-like parton in the proton and nothing else happens, has to be modified. The probability that additional partons, particularly gluons, are radiated increases with decreasing  $x$ . An example, where a low  $x$  parton, which interacts with the photon, originates from a parton shower initiated by a gluon with large  $x$ , is shown in Fig. 1. In the approximation of just one gluon being radiated in the initial or the final state, such processes have been calculated in next to leading order (NLO). Two programs, MEPJET<sup>1</sup> and DISENT<sup>2</sup>, using different methods, are available, and a new program, DISASTER++<sup>3</sup>, has been announced at this meeting. These programs generate partons only; no full event generators exist.

In the leading log approximation any number of more or less collinear or soft gluons may be radiated. By resumming terms of the form  $(\alpha_s \ln \frac{Q^2}{Q_0^2})^n$  using the DGLAP<sup>4</sup> evolution equations an initial state parton shower may be evolved from the scale  $Q_0^2$ , typically between 0.3 and 4.0 GeV<sup>2</sup>, to the scale  $Q^2$ , where the interaction with the photon takes place. DGLAP evolution

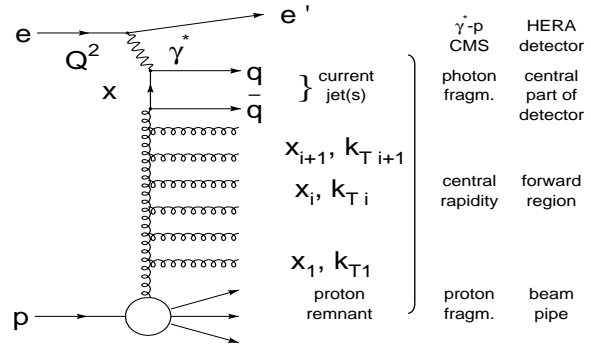


Fig. 1. Diagram of an  $ep$  collision at low  $x$ .

\*To appear in Proc. of "New Trends in HERA Physics", Ringberg, Tegernsee, Germany, May 1997.

implies weakly ordered fractional gluon energies (longitudinal momenta)  $x_i > x_{i+1}$  and strongly ordered gluon virtualities or transverse gluon momenta  $k_{T,i} \ll k_{T,i+1}$  along the ladder (Fig. 1). Different implementations of “DGLAP-like” parton showers and of matching <sup>5,6</sup> them to leading order (LO) exact matrix elements for the QCD-Compton (QCDC) and the boson-gluon fusion (BGF) process exist in LEPTO <sup>7</sup>, RAPGAP <sup>8</sup>, and HERWIG <sup>9</sup>. For the hadronisation of the perturbative partons to the observable hadrons, these programs include phenomenological models. HERWIG uses the cluster model <sup>10</sup>; all other programs, including ARIADNE <sup>11</sup>, use the LUND string model <sup>12</sup>, as implemented in the JETSET <sup>13</sup> code. These fragmentation models have been well tested at LEP <sup>14</sup>. At HERA and at hadron colliders, the additional complication of proton remnant fragmentation arises, about which much less is known.

At low  $x$ , terms of the form  $(\alpha_s \ln \frac{1}{x})^n$  become large and can be resummed using the BFKL <sup>15</sup> evolution equations. In a physical gauge, these terms correspond to a ladder diagram in which gluon emissions are strongly ordered in energies  $x_i \gg x_{i+1}$ , while, in contrast to the DGLAP case, the transverse gluon momenta perform a random walk along the ladder. Analytical results at the parton level and first results including fragmentation functions exist and will be mentioned later. Unfortunately no implementations of “BFKL-like” parton showers are available in any of the event generators.

Finally we discuss ARIADNE <sup>11</sup>, which currently gives the best overall description of the hadronic final state in DIS, but which does not fit well into any of the schemes mentioned above. It is based on the color dipole model (CDM) <sup>16</sup>, where gluon emission originates from a color dipole stretched between the scattered quark and the proton remnant. Further gluon emission leads to a chain of independently radiating dipoles spanned between color-connected partons. The first emission is corrected by the QCDC matrix element in LO. In ARIADNE, the color charge of the proton remnant is assumed not to be point-like, leading to a phenomenological suppression of gluon radiation <sup>11</sup> in the remnant direction. The suppression sets in for hard gluons with wavelengths smaller than the size of the remnant. Also the color charge of the scattered quark is taken to be spread out, depending on the virtuality  $Q^2$  of the photon <sup>11,17</sup>. This in turn leads to a suppression of radiation in the direction of the scattered quark. An important feature of ARIADNE is that the probability for a QCDC event and for any other gluon emission, from a dipole connected to the remnant at one end, depends on this “unorthodox suppression” <sup>18</sup>, due to the extended color charge, while in “normal” QCD, as implemented in all other programs, it depends on the ratio of parton densities before and after the emission and on other factors which are the same for all programs. At low  $x$  this feature leads to a greatly enhanced rate of QCDC events compared to the other generators. Additionally, in contrast to the DGLAP-like programs, the gluons in ARIADNE are not ordered in  $k_t$  along the ladder. It has therefore been argued <sup>19</sup> that the partonic final state of ARIADNE is more closely related to the one expected from BFKL evolution.

It has been shown that all models provide a fair description of basic event properties<sup>20,21,22</sup>.

At very low  $x$  the gluon density may possibly become so high in regions (“hot spots”) of the proton that the gluons will no longer act as free particles but will interact with each other. In this saturation regime of QCD, the strong coupling is still small, but the incoherent scattering approximation is no longer valid. It is not clear whether this new regime could be observed at HERA.

What do we expect to see at HERA? Which observables will be most sensitive to the underlying parton dynamics?

As  $x$  decreases below  $10^{-3}$  we anticipate deviations from the DGLAP predictions due to the missing  $(\alpha_s \ln \frac{1}{x})^n$  terms. The most inclusive way to study the structure of the proton is to measure the probing lepton after the interaction. The resulting measurement of the proton structure function  $F_2$  has the advantages that it is experimentally relatively easy and that it can be directly compared to analytical QCD calculations. The rise of  $F_2$  with decreasing  $x$  as observed at HERA<sup>23</sup> turns out to be well describable by the DGLAP evolution equations alone, down to  $Q^2 \geq 1.0 \text{ GeV}^2$  and  $x \geq 10^{-5}$ . At this meeting, it was shown that the  $F_2$  data at small  $x$  are also well compatible with a unified BFKL and DGLAP description<sup>24</sup>.

Perhaps  $F_2$  is not sufficiently sensitive to observe the change in parton dynamics at low  $x$ . The reasons might be that  $F_2$  is a too inclusive measurement, averaging out over differences only visible in the details of the hadronic final state. There might not be enough range in  $x$  at moderate  $Q^2$ . Moreover, the theory has some flexibility due to the freedom of choice of the starting parton distributions.

A greater sensitivity to small  $x$  effects might be provided by observables based on the hadronic final state emerging from the underlying partons. It can be further enhanced by making use of the differences between the DGLAP and the BFKL cascade. However, there is a price to pay. The measurements have to be compared to Monte Carlo simulations including the QCD effects, the transition from partons to hadrons, the particle decays, and detector effects. The observables studied so far are the transverse energy flows, single particle  $p_T$ -spectra, and forward jets.

## 2. Transverse Energy Flows

BFKL dynamics predicts<sup>25,26</sup>, due to the lack of ordering of  $k_T$  in the parton cascade, more average transverse energy  $E_T$  and harder tails in the  $E_T$  distribution for decreasing  $x$  than in the DGLAP scenario. These observables are measured calorimetrically in the central rapidity<sup>a</sup> region, between the struck quark and the proton remnant, in the hadronic center of mass (hcms), that is the rest system of the exchanged virtual photon and proton. In that frame all  $E_T$ <sup>b</sup> is due to either QCD

<sup>a</sup>Rapidity is here always pseudo-rapidity, i.e.  $\eta = -\ln \tan(\theta/2)$ .

<sup>b</sup> $E_T = \sum E_i \sin \theta_i$ ,  $i$  runs over calorimeter cells.

radiation or hadronisation. As indicated in Fig. 1 the central rapidity in the hcms corresponds to the forward region in the frame of the HERA detectors.

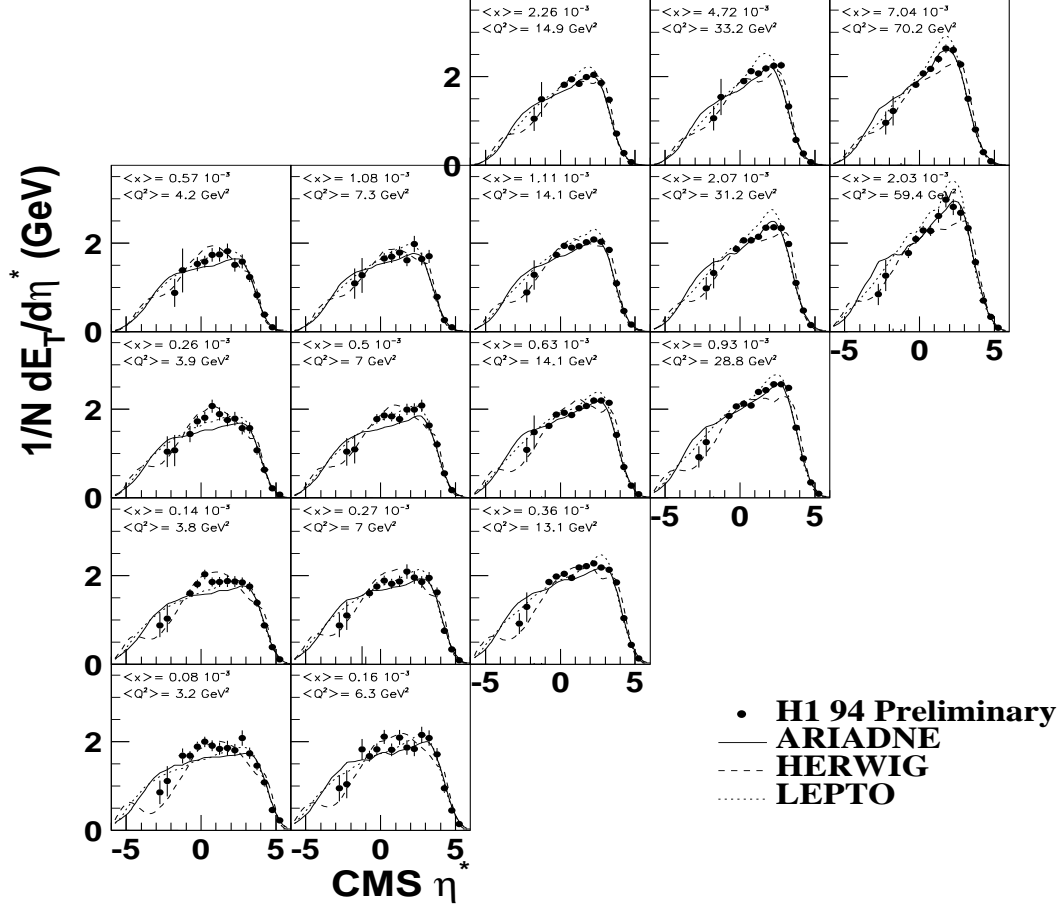


Fig. 2. Transverse energy flow as a function of rapidity  $\eta^*$  in the hcms. The H1 data points show statistical errors only, except for two points measured with the plug calorimeter where the statistical and systematic errors are given. The lines are the Monte Carlo predictions of three different models.

First results on the  $E_T$ -flows have been published by the H1 collaboration<sup>27,28,29</sup>. In ref.<sup>29</sup> they have been reported for DIS events with  $5 \text{ GeV}^2 < Q^2 < 50 \text{ GeV}^2$  and with  $10^{-4} < x < 10^{-2}$  in the hcms and have been compared to the then current model predictions of LEPTO 6.1 and ARIADNE 4.03. In the largest  $x$  and  $Q^2$  bin, i.e.  $x \approx 5 \cdot 10^{-3}$  and  $Q^2 \approx 33 \text{ GeV}^2$ , the data and the two models were found to agree. With decreasing  $x$  for fixed  $Q^2$  the  $E_T$  from LEPTO 6.1 was found to fall more and more below the data for rapidities away from the current jet, while ARIADNE 4.03 still managed to give a level of  $E_T$  in agreement with the data.

At this point in time one could have had the impression that models with DGLAP-like dynamics like LEPTO fail to describe the data at low  $x$ , while models with some

BFKL-like features like ARIADNE are successful. However, soon after, two new phenomenological features have been added to LEPTO which allowed a reasonably good description of the transverse energy flows also for decreasing  $x$ . The new features are soft color interactions<sup>30</sup>, with the intention to describe rapidity gap events without modeling a Pomeron and its structure function, and a modified sea-quark/remnant treatment, giving a smoother transition from BGF events to events where the photon interacts with a sea-quark.

The H1 collaboration in the meantime has produced new preliminary data<sup>31,32</sup>, covering a larger range in the kinematic plane from  $3 < Q^2 < 70 \text{ GeV}^2$  and  $8 \times 10^{-5} < x < 7 \times 10^{-3}$ . The extension to lower  $Q^2$  was achieved by analysing data from special runs, where the point of the  $ep$  interactions was shifted from the nominal position in the direction of the proton beam in order to have access to smaller lepton scattering angles. In addition, the  $E_T$  at two very forward rapidity bins was measured by H1 using their plug calorimeter ( $0.72^\circ < \theta_{lab} < 3.3^\circ$ ), which closes the gap between the beam-pipe and the forward part of their liquid Argon calorimeter.

The data as a function of rapidity<sup>c</sup> in the hcms are shown in bins of  $x$  and  $Q^2$  in Fig. 2. They are compared to predictions from ARIADNE 4.08, HERWIG 5.8, and LEPTO 6.4. The models give only a fair description of the data over the large range in  $x$  and  $Q^2$ . The average  $E_T$  in the central rapidity  $-0.5 < \eta^* < 0.5$  as a function of  $x$  in bins of fixed  $Q^2$  increases with decreasing  $x$ <sup>31,32</sup>. This is demonstrated in Fig. 3a for the bin  $Q^2 = 14 \text{ GeV}^2$ , together with data from ZEUS<sup>33</sup>, and with predictions from

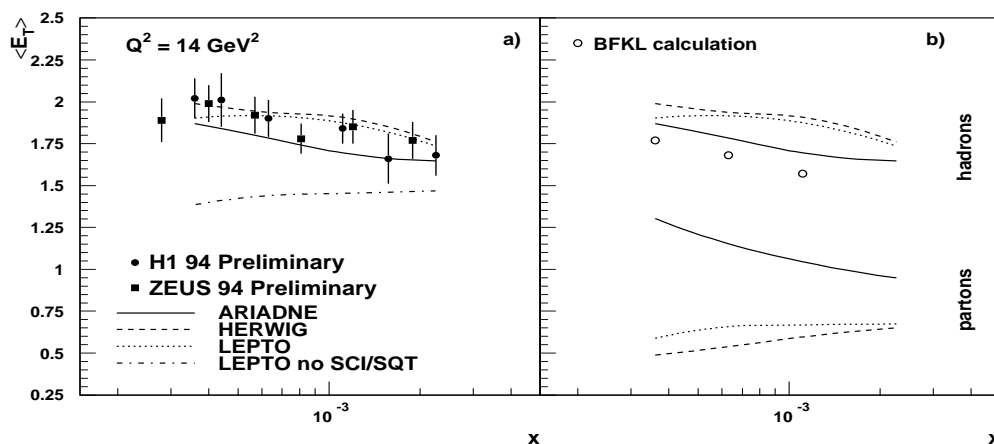


Fig. 3. Mean transverse energy in the central rapidity bin in the hcms for the bin  $Q^2 = 14 \text{ GeV}^2$ . Besides the data from H1 and ZEUS, QCD model predictions (lines) are shown for hadrons in a) and for partons in b). An analytic BFKL calculation at the parton level is shown as open circles.

different generators at the hadron level. For LEPTO the predictions are shown with the new soft color interactions (SCI) and the new sea-quark treatment (SQT) turned on and off. The data of both experiments are in good agreement and can be described

<sup>c</sup>The direction of the proton is to the left (negative rapidity).

by all models, DGLAP and BFKL-like. In Fig. 3b the predictions of the models at the hadron level are contrasted with those at the parton level and with an analytic parton level BFKL calculation<sup>25</sup>. At the parton level the DGLAP-like models LEPTO and HERWIG show the opposite slope in  $x$  than ARIADNE, the BFKL calculation, the hadron level of all models, and the data. The BFKL calculation gives the highest transverse energy, 40% to 50% above the partons from the color dipole model. There are large differences in the contribution from fragmentation to the total  $E_T$  between the models. It is about 15% for the BFKL calculation (comparing it to data), 35% for ARIADNE, and about 70% for LEPTO and HERWIG.

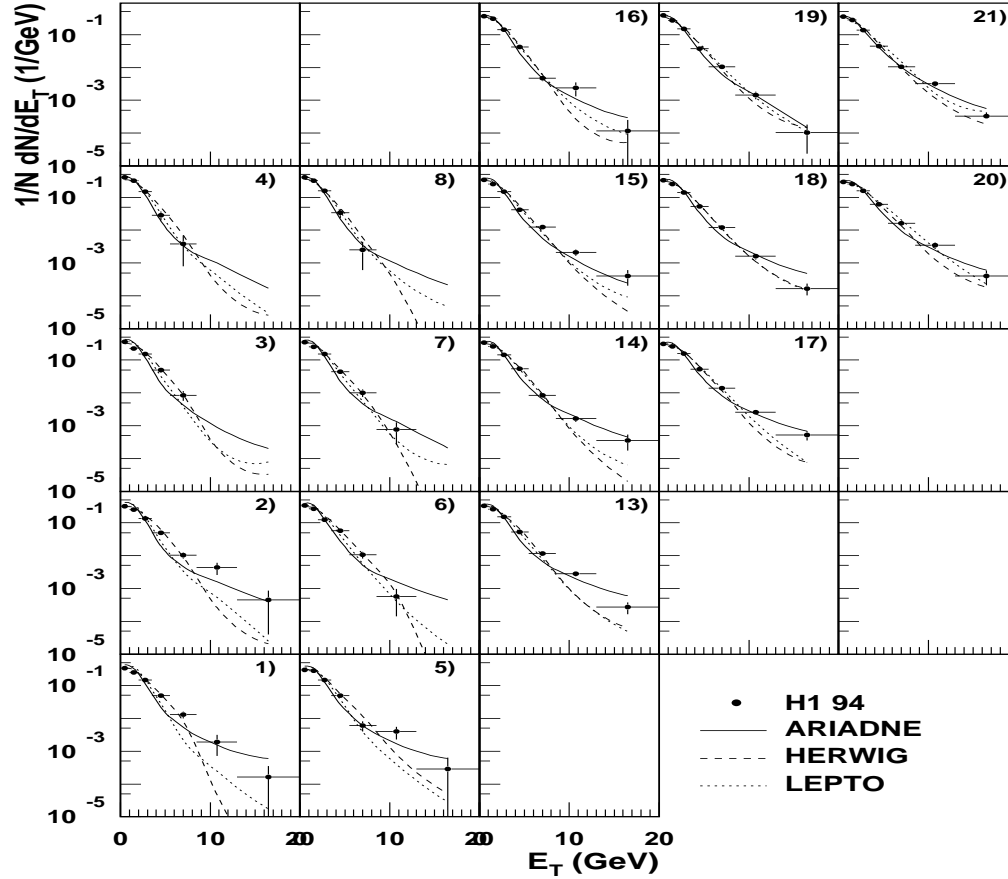


Fig. 4. Transverse energy distribution in the central rapidity bin in the hcms. Only statistical errors are shown.

Concerning the measurement of the mean  $E_T$  in the central rapidity bin, we are now in the situation that all models describe the data. Although the models differ in their underlying parton dynamics, the mean  $E_T$  can be made to agree by exploiting as yet unconstrained variations in hadronisation models.

Another observable investigated by H1 is the distribution of the  $E_T$  in the central rapidity bin per event. The  $E_T$  originating from hadronisation is expected to be limited, while high values of  $E_T$  are more likely to be produced by hard parton

radiation. Preliminary data <sup>31,32</sup>, in the same bins of  $x$  and  $Q^2$  as in Fig. 2, are displayed in Fig. 4 together with predictions from ARIADNE 4.08, HERWIG 5.8, and LEPTO 6.4. While at the largest  $x$  and  $Q^2$  the data and the models agree, with decreasing  $x$  and  $Q^2$  the data and ARIADNE appear to exhibit harder tails than the DGLAP-like models. As can be seen from the figure a firm conclusion can only be drawn with more statistics extending the range in  $E_T$  to larger values. Comparing the  $E_T$  distribution for the highest and lowest  $x$  value for fixed  $Q^2$ , one finds that the data have harder tails <sup>31,32</sup> with decreasing  $x$ , suggesting a rise in parton activity.

### 3. Single Particle $p_T$ Spectra

The  $E_T$  measured by the calorimeter can be due to many soft particles, predominantly from hadronisation, or due to a few hard particles, mainly from hard gluon emission, or due to both. Therefore it has been suggested <sup>34</sup> that the hard tail of the

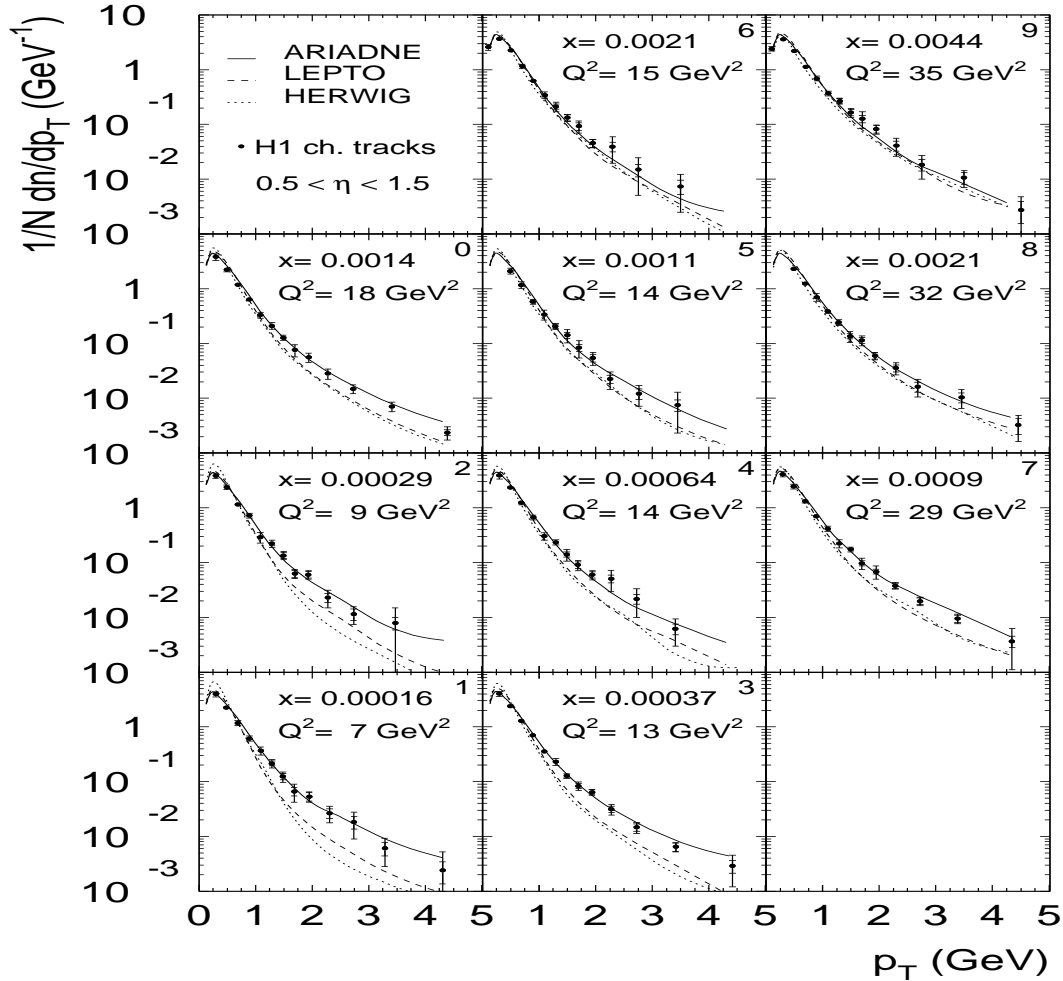


Fig. 5. The transverse momentum spectra of charged particles in the hcms. The data are shown for nine different kinematic bins and the combined sample (bin 0). Statistical and full errors are given.

$p_T$  distribution of single charged particles in the hcms might offer better sensitivity to the basic parton dynamics since it is more directly linked to hard gluon emissions.

The charged particle  $p_T$  distributions in bins of  $x$  and  $Q^2$  as measured by H1<sup>35</sup> in the rapidity interval from 0.5 to 1.5 are shown in Fig. 5. At large  $x$  all three models presented agree with the data. With decreasing  $x$ , LEPTO and HERWIG significantly fall below the data for increasing  $p_T$ . Predictions<sup>36</sup> based on BFKL resummation and convolution with fragmentation functions for the transition from partons to charged hadrons<sup>37</sup> have been made for the three lowest bins in  $x$ , i.e. bins 1, 2, and 3. As demonstrated in Fig. 6 for bin 3, the data and the BFKL result agree quite well for  $p_T \geq 1.5$  GeV. The absolute normalization was derived from a comparison of the BFKL calculation of the forward jet cross section with data from H1 to be discussed later. Also displayed in the figure is the calculation with BFKL effects turned off, which falls below the data. It is apparent from the figure

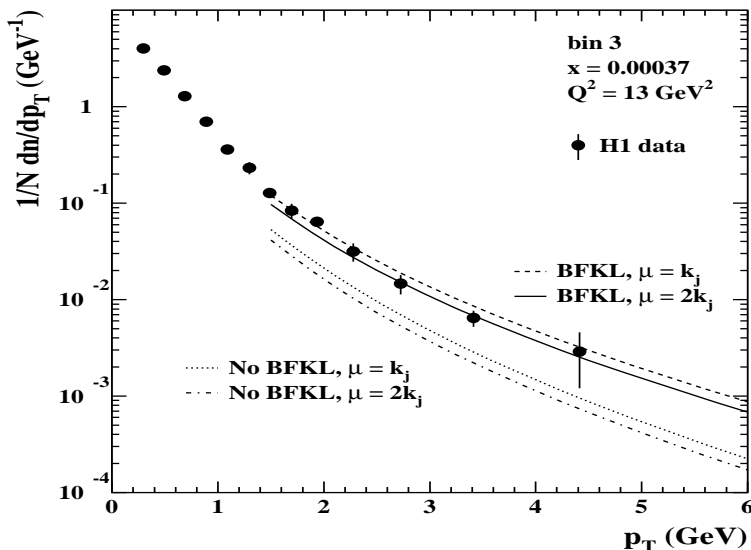


Fig. 6. The transverse momentum spectra of charged particles in the hcms for fixed low  $x$  and  $Q^2$  (bin 3). The data and predictions from a BFKL calculation, with BFKL effects off and on, and with two different choices for the scale  $\mu$  of the fragmentation function are compared.

that the significance of the agreement can be increased with more data at higher  $p_T$ . In addition, BFKL effects would become stronger, if the measurement of charged particles could be extended further in the direction of the proton remnant, i.e. to the rapidity interval  $-0.5 < \eta^* < 0.5$ .

#### 4. Forward Jets

The cross section for forward jets in DIS as a function of  $x$  has been advertised<sup>38</sup> for some time now as an observable enhancing the effects of BFKL resummation. Diagrammatically the situation is described in Fig. 7. The forward jet is defined by





In Fig. 8 the ZEUS forward jet cross section corrected to the parton level of ARIADNE is shown and compared to several parton level calculations: an analytic BFKL calculation <sup>43</sup>, the same calculation but without any gluon emission between the forward and the current jet system (Born BFKL), and a fixed NLO QCD calculation using MEPJET. The data show a much faster rise with decreasing  $x$  than the calculations without BFKL resummation. The BFKL calculation shows an even more dramatic rise. The authors <sup>43</sup>, however, point out that several effects which have not been taken into account might lower their prediction. ZEUS presents their preliminary result corrected to the parton level in order to compare to parton level calculations. Using ARIADNE correction factors are found to vary between 0.6 for the lowest  $x$  bin and  $\approx 1$  for larger  $x$ . It will be useful to have the ZEUS cross section also at the hadron level, since it is not clear, what the relationship is between the parton level of the CDM and BFKL. It could also allow comparisons with H1 data which are corrected to the hadron level.

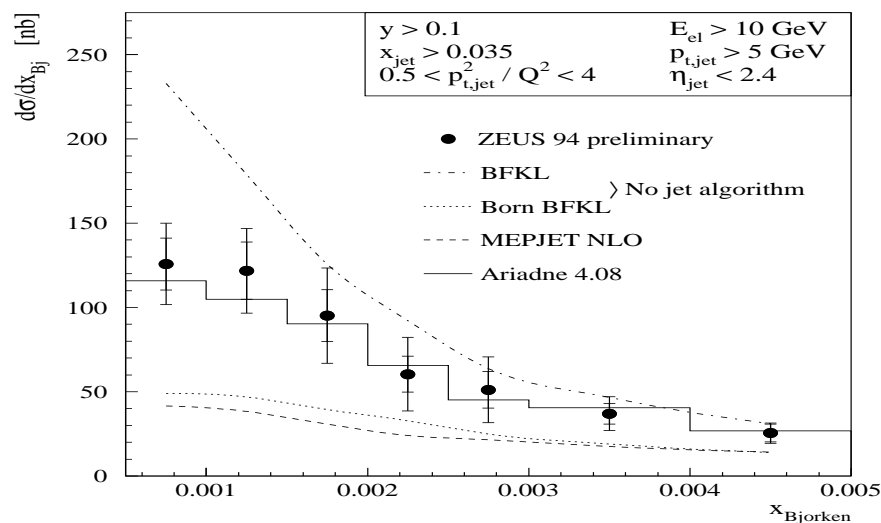


Fig. 8. The differential forward jet cross section as a function of  $x$ . The ZEUS data have been corrected to the parton level. Statistical and systematic errors (not yet complete) are included. BFKL calculations, with BFKL effects on (dash-dotted line) and off (dotted line), calculations in NLO QCD using MEPJET, and parton level results from the color dipole model are shown.

The preliminary H1 results on the forward cross section are shown in Fig. 9a and are compared to predictions from LEPTO (MEPS) with and without soft color interactions (SCI) and to ARIADNE (CDM). Again a fast rise of the cross section is observed with the CDM falling only slightly below the data. In Fig. 9b models and calculations at the parton level are shown: ARIADNE, LEPTO, two BFKL calculation <sup>43,36</sup>, and a NLO calculation using DISENT. ARIADNE shows a similar  $x$  dependence at the parton and hadron level with hadronisation effects amounting to less than 20%. The parton level forward jet cross sections of LEPTO and of

DISENT in NLO agree as expected and show a moderate increase. In LEPTO, with soft color interactions turned on, up to 80% of the forward jets are created in the hadronisation phase causing LEPTO to only slightly undershoot the data with decreasing  $x$ . The BFKL calculations basically can only predict the dependence on  $x$  but not the normalization. As mentioned before, the computation by Kwiecinski et al.<sup>36</sup> fixed the normalization to the data from H1 while the calculation by Bartels et al.<sup>43</sup> did not. Scaling the cross section by Bartels et al. down by a factor 0.8 brings the two BFKL calculations in agreement. The color dipole model provides the

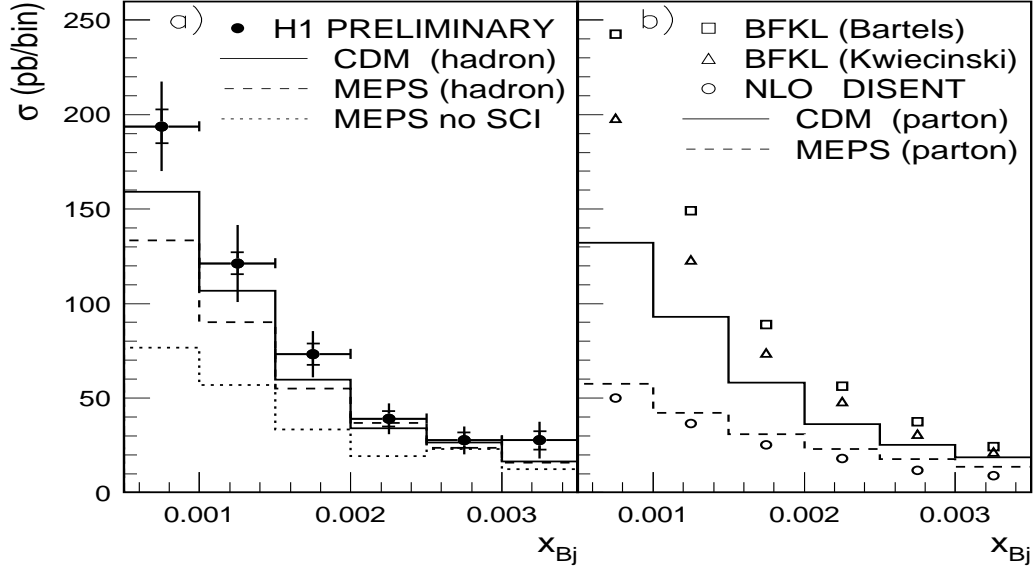


Fig. 9. The forward jet cross section as a function of  $x$ . The H1 data have been corrected to the hadron level. Statistical and systematic errors are included. QCD model predictions for hadrons are superimposed in (a) and for partons in (b). Two analytic BFKL calculation (open squares and triangles) and a NLO calculation using DISENT (open circles) are also shown in (b).

best description of the data. However, it should be pointed out that its prediction is rather sensitive to the power of soft suppression of gluon emission  $(\mu/p_T)^\alpha$  due to the proton remnant. The parameter  $\alpha$  is related to the dimensionality of the extended proton remnant and is expected to be  $\approx 1$ . The H1 forward jets prefer  $\alpha \leq 1.0$  while non-jet observables like energy flows prefer  $\alpha \approx 1.5$ <sup>20</sup>.

One may wonder about the choice for the minimum  $p_{Tjet}$ , 3.5 GeV by H1 and 5.0 GeV by ZEUS. A small value is desirable from the point of view of statistics and sensitivity to BFKL effects<sup>44</sup>. With increasing  $p_{Tjet}$  the slope in  $x$  for the forward jet cross section decreases. The requirement  $p_{Tjet} \approx Q^2$  forces the  $Q^2$  to increase, which in turn increases the minimum  $x$  which is probed. On the other hand, to suppress hadronisation effects, one would want  $p_{Tjet}$  to be large.

Another question concerns the choice of the upper limit on  $p_{Tjet}^2/Q^2$  which is 2.0 for H1 and 4.0 for ZEUS. Increasing this limit from 2.0 to 4.0 increases in the lowest

$x$  bins the contribution from  $O(\alpha_s)$  matrix elements to the forward jets by roughly a factor of two. One would also expect an increased contribution from resolved photoproduction which is not included in the calculations. After this workshop the author of RAPGAP has shown <sup>45</sup> that for example the H1 result can also be described with direct (same as in LEPTO without SCI) and resolved contributions.

## 5. Conclusions

The tails of the single particle  $p_T$  spectra and of the calorimetric  $E_T$  distribution, and the forward jet cross sections offer a good chance to pin down deviations from the DGLAP paradigm. Other interesting observables in this quest, like the decorrelation of the azimuthal angle between the forward jet and the lepton <sup>43</sup>, the forward  $\pi^\circ$  cross section <sup>46</sup>, and the production of more than one forward jet <sup>47</sup> should be pursued.

Along the way, we probably will and have to get a better understanding of hadronisation effects, particularly of the proton remnant. On the theory side, higher order effects <sup>48</sup> have to be included in the calculations and a BFKL Monte Carlo generator <sup>49,50</sup> is needed.

In addition to collecting more data at HERA, it would be desirable to access smaller forward angles for jets <sup>44</sup> and particles and to increase the HERA center of mass energy.

## 6. Acknowledgements

I want to thank T. Carli, M. Wobisch, and S. Wölflé for providing me with plots and J. Dainton, J. Hartmann, and D. Krücker for a careful reading of the manuscript. I am also happy to thank the organizing committee, in particular B. Kniel, for the excellent workshop and the pleasant atmosphere.

## 7. References

1. E. Mirkes and D. Zeppenfeld, Phys. Lett. B380 (1996) 205.
2. S. Catani and M. Seymour, Proc. Workshop on Future Physics at HERA 1995/96, Hamburg, eds. G. Ingelman, A. De Roeck, and R. Klanner, vol. 1 (1996) 519, CERN-TH/96-240 (1996) [hep-ph/9609521], and Acta Phys. Polon. B28 (1997) 863.
3. D. Graudenz, these proceedings.
4. V.N. Gribov and L.N. Lipatov, Sov. J. Nucl. Phys. 15 (1972) 438 and 675; G. Altarelli and G. Parisi, Nucl. Phys. B126 (1977) 298; Yu.L. Dokshitzer, Sov. Phys. JETP 46 (1977) 641.
5. M. Bengtsson, G. Ingelman, and T. Sjöstrand, Proc. HERA Workshop 1987, Hamburg, ed. R.D. Peccei, vol. 1 (1988) 149;

- M. Bengtsson and T. Sjöstrand, Z. Phys. C37 (1988) 465.
6. M. H. Seymour, LU-TP-94-12, Nucl. Phys. B436 (1995) 443 and Comput. Phys. Commun. 90 (1995) 95.
  7. G. Ingelman, Proc. Workshop on Physics at HERA 1991, Hamburg, eds. W. Buchmüller and G. Ingelman, vol. 3 (1992) 1366;  
G. Ingelman, A. Edin, and J. Rathsman, Comput. Phys. Commun. 101 (1997) 108.
  8. H. Jung, Comput. Phys. Commun. 86 (1995) 147.
  9. G. Marchesini et al., Comput. Phys. Commun. 67 (1992) 465.
  10. B.R. Webber, Nucl. Phys. B238 (1984) 492;  
G. Marchesini and B.R. Webber, Nucl. Phys. B310 (1988) 461.
  11. L. Lönnblad, Comput. Phys. Comm. 71 (1992) 15 and Z. Phys. C65 (1995) 285.
  12. B. Andersson, G. Gustafson, G. Ingelman, and T. Sjöstrand, Phys. Rep. 97 (1983) 31.
  13. T. Sjöstrand, Comput. Phys. Commun. 82 (1994) 74;  
T. Sjöstrand, PYTHIA 5.7 and JETSET 7.4, CERN-TH 7112/93 (1993) and LU TP 95-20 (1995).
  14. I. G. Knowles et al., Proc. LEP2 Physics Workshop 1995 [hep-ph/9601212].
  15. E. A. Kuraev, L. N. Lipatov, and V. S. Fadin, Sov. Phys. JETP 45 (1977) 199;  
Ya. Ya. Balitsky and L. N. Lipatov, Sov. J. Nucl. Phys. 28 (1978) 822.
  16. G. Gustafson, Phys. Lett. B175 (1986) 453;  
G. Gustafson and U. Petterson, Nucl. Phys. B306 (1988);  
B. Andersson, G. Gustafson, L. Lönnblad, and U. Petterson, Z. Phys. C43 (1989) 625.
  17. L. Lönnblad, M. Seymour, et al., Proc. Physics at LEP 2 Workshop, eds. G. Altarelli, T. Sjöstrand, and F. Zwirner, CERN/96-01, vol. 2, (1996) 187.
  18. J. Rathsman, Phys. Lett. B393 (1997) 181.
  19. A.H. Mueller, Nucl. Phys. B415 (1994) 373.
  20. N. Brook et al., Proc. Workshop on Future Physics at HERA 1995/96, Hamburg, eds. G. Ingelman, A. De Roeck, and R. Klanner, vol. 1 (1996) 613.
  21. T. Carli, Proc. 4th Int. Workshop on Deep Inelastic Scattering and Related Phenomena (DIS 96), Roma, eds. G. D'Agostini and A. Nigro, (1997) 415.
  22. H. Jung, private communication.
  23. L. Favart, these proceedings.
  24. A.D. Martin, these proceedings.
  25. K. Golec-Biernat, J. Kwiecinski, A.D. Martin, and P.J. Sutton, Phys. Rev. D50 (1994) 217 and Phys. Lett. B335 (1994) 220.
  26. J. Bartels, H. Lotter, and M. Vogt, Phys. Lett. B373 (1996) 215.
  27. H1 Collaboration, T. Ahmed et al., Phys. Lett. B298 (1993) 469.
  28. H1 Collaboration, I. Abt et al., Z. Phys. C63 (1994) 377.

29. H1 Collaboration, S. Aid et al., Phys. Lett. B356 (1995) 118.
30. A. Edin, G. Ingelman, and J. Rathsman, Z. Phys. C75 (1997) 57 and Phys. Lett. B366 (1996) 371.
31. H1 Collaboration, C. Adloff et al., contrib. paper pa02-073, ICHEP '96, Warsaw, Poland, July 1996.
32. M. F. Hess, Ph.D. Thesis, University of Hamburg (1996).
33. N. A. Pavel, Proc. 4th Int. Workshop on Deep Inelastic Scattering and Related Phenomena (DIS96), Roma, eds. G. D'Agostini and A. Nigro, (1997) 502.
34. M. Kuhlen, Phys. Lett. B382 (1996) 441.
35. H1 Collaboration, C. Adloff et al., Nucl. Phys. B485 (1997) 3.
36. J. Kwiecinski, S.C. Lang, and A.D. Martin, DTP-97-56 (1997) [hep-ph/9707240].
37. J. Binnewies, B. A. Kniehl, and G. Kramer, Phys. Rev. D52 (1995) 4947.
38. A.H. Mueller, Nucl. Phys. B (Proc. Suppl.) 18C (1990) 125 and J. Phys. G17 (1991) 1443;  
W.K. Tang, Phys. Lett. B278 (1992) 363;  
J. Bartels, A. De Roeck, and M. Loewe, Z. Phys. C54 (1992) 635;  
A. De Roeck, Nucl. Phys. B (Proc. Suppl.) 29A (1992) 61;  
J. Kwiecinski, A.D. Martin, and P. J. Sutton, Phys. Lett. B287 (1992) 254, Nucl. Phys. B (Proc. Suppl.) 29A (1992) 67, and Phys. Rev. D46 (1992) 921.
39. J. G. Contreras, Proc. XXXI Rencontres de Moriond in QCD and High Energy Hadronic Interactions, ed. J. Tran Thanh Van, Edition Frontieres (1996) 411; H1 Collaboration, C. Adloff et al., contrib. paper pa03-049, ICHEP '96, Warsaw, Poland, July 1996.
40. S. Wölflé, to be published in Proc. 5th Int. Workshop on Deep Inelastic Scattering and QCD, Chicago, April 1997, eds. D. Krakauer and J. Respond.
41. J. G. Contreras, Ph.D. Thesis, University of Dortmund (1997).
42. E. M. Lobodzinska, Ph.D. Thesis, Inst. of Nucl. Physics, Cracow (1997).
43. J. Bartels et al., Phys. Lett. B384 (1996) 300.
44. J. Bartels, A. De Roeck, and M. Wüsthoff, Proc. Workshop on Future Physics at HERA 1995/96, Hamburg, eds. G. Ingelman, A. De Roeck, and R. Klanner, vol. 1 (1996) 598.
45. H. Jung, to be published in Proc. Madrid Workshop on Low  $x$  Physics, Miraflores de la Sierra, June 1997.
46. J. Kwiecinski, S. C. Lang, and A. D. Martin, Phys. Rev. D55 (1997) 1273.
47. J. Kwiecinski, C. A. M. Lewis, and A. D. Martin, DTP-97-58 (1997) [hep-ph/9707375].
48. J. Bartels, these proceedings.
49. C. R. Schmidt, Phys. Rev. Lett. 78 (1997) 4531.
50. L. H. Orr and W. J. Stirling, DTP-97-48 (1997) [hep-ph/9706529], to be published in Phys. Rev. D.